Edelweiss Applied Science and Technology

ISSN: 2576-8484 Vol. 9, No. 10, 1552-1566 2025 Publisher: Learning Gate DOI: 10.55214/2576-8484.v9i10.10701 © 2025 by the authors; licensee Learning Gate

Calculation of biomass of individual trees on a combination of ground, aerial laser scanning and multispectral imagery from an unmanned aerial vehicle

©Veronika Kostyk¹*, ©Kirill Kalashnikov², ©Konstantin Nagornyi¹,², Evgeny Lialiushko², ©Snezhana Vikhrenko¹, ©Valentina Kalinkina¹, ©Angelika Demina¹

¹Institute of the World Ocean, Far Eastern Federal University, Russian Federation; kostyk.va@dvfu.ru (V.K.) nagornyi.ka@dvfu.ru (K.N.) vikhrenko.sv@dvfu.ru (S.V.) kalinkina.va@dvfu.ru (V.K.) demina.as@dvfu.ru (A.D.).

²Polytechnic institute, Far Eastern Federal University, Russian Federation; kalashnikov.ki@dvfu.ru (K. K.) lialiushko.ea@dvfu.ru (E.L.).

Abstract: Biomass is a key indicator for monitoring the global carbon cycle. Parameters of individual tree species in mixed forests are crucial for forestry, but research mainly focuses on forests dominated by a single species. The issue of biomass estimation in mixed forests remains underexplored. This study determined the biomass of various tree species in a mixed forest by integrating aerial and ground scanning data with multispectral aerial imagery. The study involved classifying trees using multispectral data combined with field surveys on a test plot, merging results from ground and aerial surveys, and using point clouds to measure tree diameter and height. Results indicate that with specialized processing of multispectral images, tree species can be identified with 63% accuracy, and individual tree biomass can be calculated using laser scanning data. Comparisons of tree diameters and heights from laser scanning and field measurements showed maximum discrepancies of 11%. Tree heights measured from point clouds were more accurate than field measurements, while trunk diameters from scanning and field data showed similar accuracy.

Keywords: Aerial photography, Biomass, Laser scanning, Tree diameter, Tree height.

1. Introduction

Carbon dioxide emissions have increased significantly over the past century, leading to gradual global climate change and environmental degradation [1]. It is known that terrestrial ecosystems can effectively reduce carbon dioxide emissions through photosynthesis. Forests are the largest carbon storage facilities on land, which effectively control emissions by regulating the global carbon cycle and slowing climate change [2]. Therefore, accurate and prompt determination of forest biomass is especially important. New and fast methods for calculating biomass are essential for environmental monitoring, forest management, and decision-making on the climate agenda.

Traditional methods for determining tree height and trunk diameter are based on field measurements. At the same time, the height and diameter of the tree are difficult parameters to determine, since measurements are often performed in conditions of rugged terrain, dense vegetation, and they strongly depend on the experience of the performer. Thus, traditional forest inventory is a laborious and largely subjective task [3].

The development of unmanned aircraft, inertial positioning systems, GNSS (Global Navigation Satellite System) technologies, and the emergence of various UAV (Unmanned Aerial Vehicle) payloads open up new opportunities in remote sensing of forests. At the same time, photogrammetric image processing and computer vision technologies are being improved, allowing for detailed analysis of forest areas [4].

Many scientific publications have been devoted to the issue of determining forest biomass based on remote sensing data using UAVs. To determine the metric characteristics of the trees, researchers use the results of ground and aerial laser scanning. Thus, in Anjin et al. [5], based on the results of aerial laser scanning (LiDAR – Light Detection and Ranging), a cloud of laser reflection points was obtained, which provides a qualitative basis for generating data on the height and diameter of trees. Information was obtained on the configuration of the upper part of the tree trunk and the boundaries of the projective crown cover, enabling the determination of biomass and comparison with field data.

Borsah et al. [6], in their article, the authors described methods for selecting metrics for modeling biomass and considered various evaluation criteria for choosing allometric equations to estimate aboveground forest biomass using LiDAR data. A review of the articles in this publication showed that most researchers focus on using LiDAR data for analysis at the local level.

In Cao et al. [7], the authors compare aerial photography and LiDAR data. The comparison was carried out in areas with different tree species, trunk height, and density. The results showed that the similarity between the obtained aerial photography and LiDAR data was observed in areas where the height of the trees is higher and the trunk density is lower. In the article Lisein et al. [8] a combined method was also used to model the surface of the forest canopy. The combination of digital terrain models based on aerial photography and LiDAR made it possible to determine the height of vegetation with high accuracy. The method of segmentation of individual trees based on a cloud of points obtained with LiDAR made it possible to detect 86% of the trees [9]. The article Neuville et al. [10] shows the possibility of combining data with UAV and LiDAR. The algorithm, based on the application of machine learning, has demonstrated high accuracy in determining the parameters of tree trunks.

Most researchers focus on determining the characteristics of forest lands using aerial photography data from UAVs or LiDAR [8, 10-15]. However, there are studies where ground-based laser scanning data is used as a basis. For example, in Ivanova et al. [16], the orthophoto images obtained from aerial photography were combined with ground-based laser scanning data, which made it possible to correctly detect 73% of all trees. The method used allows for the automatic selection of most trees, while the selection of coniferous trees is more accurate.

Modern research focuses on the calculation of aboveground biomass in homogeneous forests [14] to a lesser extent, publications are devoted to calculations for mixed forests. Combining aerial and ground LiDAR technologies allows for reduced resource expenditure to obtain individual characteristics of trees, even in mixed forests [8, 10, 11, 16, 17].

One of the disadvantages of aerial and ground-based laser scanning technologies for determining biomass is the need for field surveys to identify the type of plant. Multispectral and hyperspectral remote sensing data may serve as alternative data sources. Multispectral images are widely used in Earth remote sensing. They are generated using specialized sensors operating within narrow wavelength ranges of the electromagnetic spectrum. The use of multispectral sensors enables the extraction of spectral characteristics of objects and, unlike traditional cameras operating in the visible range, provides information inaccessible to human vision.

In remote sensing, satellites and unmanned aerial vehicles are most often equipped with multispectral sensors. Satellite data covers vast territories, allows for data collection even from places inaccessible to humans, and enables repeated observations at a certain frequency, depending on the parameters of the orbit. However, various atmospheric effects, including clouds, which are a laborious factor to account for and relatively low spatial resolution compared to UAVs, influence satellite data. The development of small spacecraft and their placement in low orbits can reduce the impact of these effects. Currently, only UAVs are capable of providing detailed images of small areas at specific points in time, which are only affected by weather conditions that limit UAV deployment.

Multispectral remote sensing data allows us to classify trees by species, but does not provide sufficient information about their metric characteristics. Aerial and laser scanning provide three-dimensional information about individual trees, but do not characterize the species composition of the trees.

The study proposes a combined method for determining the aboveground biomass of individual trees based on the results of ground and aerial laser scanning, as well as multispectral remote sensing data using UAVs.

The method was applied at the campus of the Far Eastern Federal University (FEFU), Vladivostok, and the results were verified based on the results of field surveys. The combined method allows for a more accurate and faster assessment of the biomass of forests and individual trees, and is suitable for local sites.

2 Materials and Methods

The research was conducted on the campus of FEFU, located on Russky Island in Peter the Great Bay (Sea of Japan). The island is separated from the mainland by the Eastern Bosphorus Strait, in Ajax Bay. The distance to Vladivostok via the strait is 800 km, to Seoul – 740 km, to Tokyo – 1000 km, and to Beijing – 1300 km.

The climate of the region is monsoon; the vegetation period lasts 170 days. The average temperature in January is -7° C, and in July, it is $+17.3^{\circ}$ C. The average annual precipitation is 853 mm. The duration of the frost period (when the air temperature is less than 0° C) is 90 days. The rate of increase in air temperature is 0.3° C per 10 years, and the amount of precipitation increases by 14.8 mm per 10 years [18].

2.1. Study Site

The study site is a mixed forest located on the territory of the carbon polygon in the park of FEFU's campus [19]. The carbon polygon includes the land area of the seaside terrace (0.04 km²) and marine water area (0.2 km²). The average altitude above sea level is 18.5 m, with height differences ranging from 39 to 2 m. Geographical coordinates are from 43°01'31" to 43°01'48" north latitude, and from 131°53'40" to 131°54'09" east longitude (Figure 1).

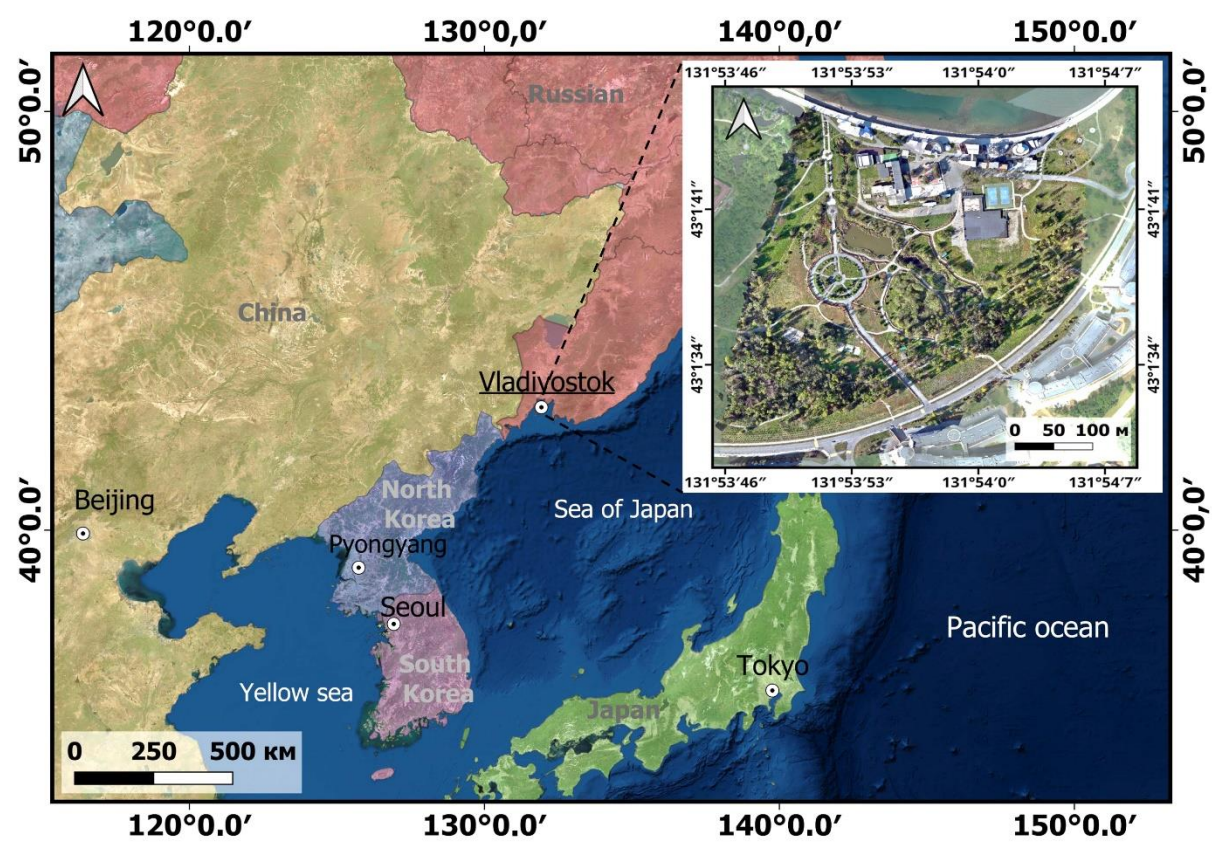


Figure 1. Location of the study site: Carbon polygon site on the campus of FEFU.

The landscape park area of the FEFU's campus includes both natural and artificial plantings. Natural landscapes are represented by broadleaf forests with a predominance of Mongolian oak. Artificial plantings consist of coniferous and deciduous species relevant in landscaping. The carbon polygon includes a section of multi-breed broadleaf forest, the species composition of which includes Mongolian oak (*Quercus mongolica* Fisch. ex Ledeb.), Manchurian ash (*Fraxinus mandshurica* Rupr.), Manchurian lime (*Tilia mandshurica* Rupr.), prickly castor oil tree (*Kalopanax septemlobus* (Thunb.) Koidz.), Amur cork tree (*Phellodendron amurense* Rupr.), Manchurian birch (*Betula pendula* subsp. *mandshurica* (Regel.) Ashburner & McAll.), and several species of the genus Salix (willows).

2.2. Field data collection

2.2.1. Natural geobotanical data

To clarify the identification of trees by ground and aerial laser scanning, a test area measuring 20*20 m (400 m²) was allocated within the polygon, on which, according to generally accepted geobotanical and forestry methods [20, 21], a complete geobotanical description was conducted in July 2025. In total, 103 species of vascular plants were recorded in the test area, including 7 trees (Table 1). Morphometric parameters (height and diameter) were determined for each tree. Diameters were measured at chest height using a measuring tape. The height of trees was measured with an altimeter Suunto (Suunto PM-5/1520). The position of trees was determined using a GNSS receiver PrinCe I90 with a positioning accuracy of ± 5 cm. Latin names of taxa are provided according to the summary «Vascular plants of the Soviet Far East» [22].

Table 1.Species composition and morphological characteristics of trees in the test area.

Species	Morphological characteristics
Kalopanax septemlobus	Large tree with dense leathery leaves, usually with 7 lobes; young shoots with shingled thorns,
	the thorns fall off as they age.
Quercus mognolica	Large tree, leaves are elongated-obovate, with blunt and entire-edged blades, glabrous or
	slightly pubescent; shoots are glabrous; the plume is thick, hemispherical, covering the acorn by
	half or a third.
Betula mandshurica	Tree with white bark; leaves are deltoid with a broadly wedge-shaped base, coarsely toothed
	along the edge; fruit catkins are solitary, drooping.
Fraxinus mandshurica	Large tree with feathery leaves consisting of 7-11 leaflets with finely sawn edges; the crown is
	high and delicate. Inflorescences are lateral and leafless. Fruits are winged.
Phellodendron amurense	A dioecious tree with thick cork bark; leaves are unpaired with a characteristic odor; feathery,
	fragrant leaves; flowers in loose panicles; juicy black fruits.
Tilia amurensis	Large tree with rounded, broad leaves, glabrous or pubescent from below; inflorescences are
	loose with numerous flowers; fruits are spherical.
Salix caprea	A tree or a tall bush with regular, large, wrinkled leaves, densely pubescent from below; catkins
-	develop before the leaves; two stamens; the ovary is pubescent.

2.2.2. Application of Remote Sensing Methods

For the study, two observation cycles were performed: March 14 (absence of active vegetation) and July 1 (active vegetation phase) in 2025. Each cycle consisted of aerial photography, aerial laser scanning, and ground-based laser scanning.

2.2.2.1. Preparatory Stage

For photogrammetric processing, control, and comparison of the results, 27 identification marks were laid on the territory of the carbon polygon (Figure 2). Identification marks were coordinated using a GNSS receiver PrinCe I 90 in RTK (Real-time kinematics) mode from the permanent GNSS base station VLDV (PrinNet network of PRIN JSC) in the UTM 52N coordinate system. Before the flight, 50x50 cm identification marks made of banner fabric were installed at the centers (Figure 2). During flight operations and ground scanning, the GNSS receiver PrinCe I90 was working in static mode with a frequency of 5 Hz at the SGN (state geodetic network) point with force centering. The subsequent processing of the aerial photography, aerial, and ground laser scanning results was performed based on static observation data in PPK (Post-processing kinematics) mode.

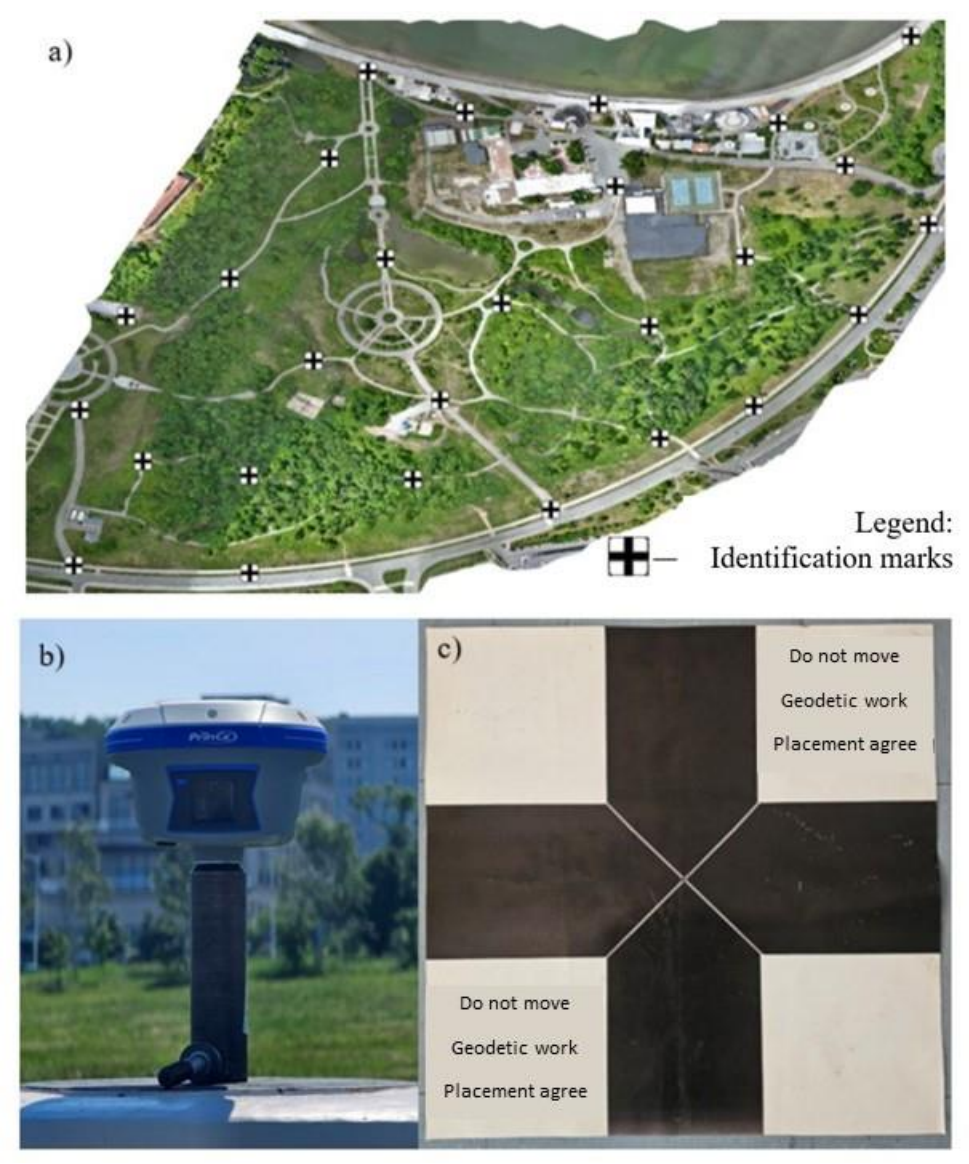


Figure 2.

Location of identification marks.

Note: a. Layout of the identification marks in the study area. b. GNSS receiver PrinCe I90 at SGN point with forced centering. c. Identification mark.

2.2.3. Multispectral Aerial Photography

Photography was performed using a UAV DJI Mavic 3 Multispectral with a primary RGB camera, a four-camera multispectral module, and an RTK module (Table 2). The flight was conducted according to a typical flight mission at an altitude of approximately 60 m, with the «following the terrain» function activated. The longitudinal and transverse overlaps of images were 80% and 70%, respectively (Figure 3).

Table 2. Characteristics of the DJI Mavic 3 Multispectral cameras.

Characteristics	RGB camera	Multispectral camera	
Image sensor	4/3" CMOS, 20 MP effective pixels	½.8-inch CMOS, 5 MP effective pixels	
Equivalent focal length	24 mm	25 mm	
Aperture	f/2.8-f/11	f/2.0	
Max image size	5280 x 3956	2592x1944	
Red band (R)	625 nm	650 nm ± 16 nm	
Green band (G)	540-570 nm	560 nm ± 16 nm	
Blue band (B)	510-540 nm	-	
Red edge band (RE)	1	730 nm \pm 16 nm	
Near infrared band (NIR)	-	860 nm ± 26 nm	

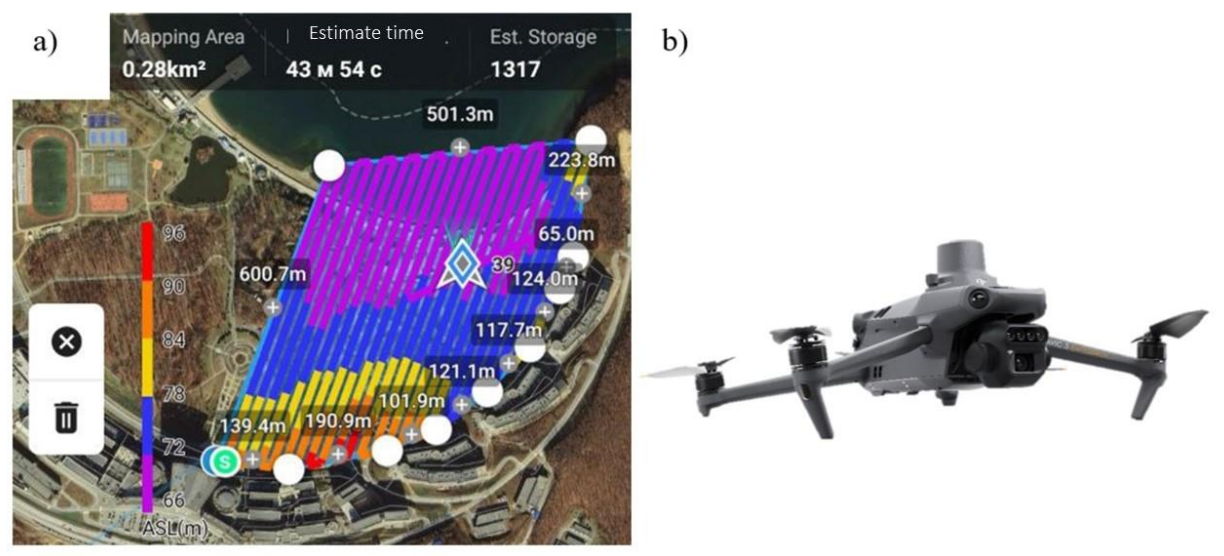


Figure 3.Multispectral aerial photography flight assignment **Note:** a. Flight mission DJI Mavic 3 Multispectral. b. UAV DJI Mavic 3 Multispectral.

Coordinates of the photographing centers were calculated in the Agisoft Metashape software. The resulting images were imported into Agisoft Metashape software and transformed into the UTM 52N coordinate system. As a result, a point cloud, digital surface model (DSM), digital elevation model (DEM), and orthophoto images with a spatial resolution of 3 cm/pixel for each of the 7 channels were obtained. The DEM is based on the earth's surface, classified on a point cloud using functions of Agisoft Metashape.

2.2.4. Unmanned Aerial Vehicle Laser Scanning

Scanning was performed using a UAV DJI Matrice 300 RTK with a Zenmuse L1 payload (Table 3). The flight was conducted at an altitude of 60 m relative to the surface, with a flight speed of 3 m/s, a scanning frequency of 160 kHz, with up to 3 echo signals, and a point density of 524×10^3 points/m². Photogrammetry for coloring the point cloud in RGB was carried out concurrently with scanning, with longitudinal and transverse overlaps of 70% and 30%, respectively (Figure 4).

Table 3.Characteristics of the DJI Zenmuse L1

Characteristics of the	ic Dai Zemnuse Di.		
Maximum	450 M (at 80%	Ranging	3 cm x 100 m
detection range	reflectivity), 0 klx	accuracy	
Point rate	Single return:	Stabilized	3-axis
	240 000 points/s	gimbal	
	Second return	FOV (field of	Non-repetitive scanning pattern: 70.4° (horizontal) × 77.2°
	240 000 points/s	view)	(vertical);
			Repetitive scanning pattern: 70.4° (horizontal) $\times 4.5^{\circ}$ (vertical)
	Third return	Laser safety	Class 1 (IEC 60825-1:2014)
	160 000 points/s		

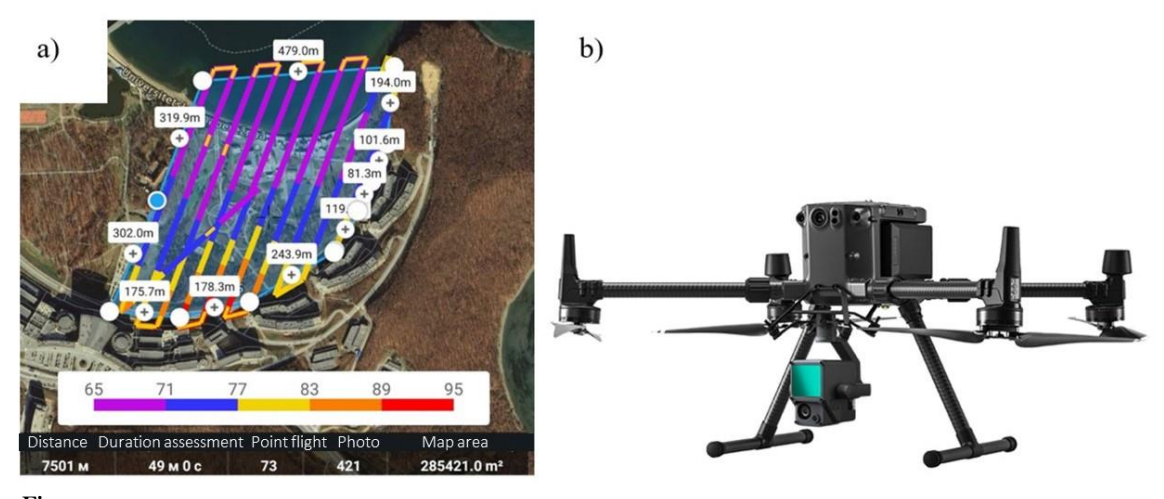


Figure 4.
Flight task of aerial laser scanning
Note: a. Flight mission DJI Matrice 300 with payload Zenmuse L1. b. DJI Matrice 300 with payload Zenmuse L1.

The primary processing of scanning results was performed in DJI Terra software in PPK mode relative to the SGN point with forced centering, with a distance between the laser scanning points of 10 cm and the UTM 52N coordinate system. The resulting point cloud was colored in RGB from photographs taken on the DJI Zenmuse L1 during laser scanning. Further processing was performed in Lidar360 software together with ground laser scanning.

2.2.4.1. Ground Laser Scanning

The data was collected using a laser scanner, GreenValley LiGrip H300. SLAM (Simultaneous Localization and Mapping) technology allows laser scanning to be performed in parallel with a working GNSS antenna, which is why the resulting point clouds are formed in the coordinate system required by the user. The relative accuracy of the obtained point clouds is ±1 cm. The point rate is 640,000 points per second, at a distance of up to 300 m (Table 4). The positioning accuracy of the RTK module is 1 cm + 1 ppm. The survey was carried out according to the PPK-SLAM principle, where the data recorded during the survey was then jointly processed with data from a permanent base GNSS station to obtain accurate motion coordinates and a positioned point cloud relative to them. The trajectory of movement varied depending on external factors but was chosen to fully cover the polygon's area (Figure 5). An important factor was to arrange the trajectory so that the operator did not cross it during scanning, as this could lead to failures and incorrect processing of the received measurements. Some areas were not fully covered due to dense vegetation threatening the integrity of the scanning head and GNSS antenna. The distance covered during the March cycle was 7.6 km and was completed in 125 minutes. In July, the trajectory was 8.3 km long and completed in 118 minutes.

Table 4. Characteristics of LiGrip H300.

Laser type	XT32M laser	Horizontal FOV (field of view)	280°
Scan rate	640 kpts/s	Vertical FOV (field of view)	3600
Relative accuracy	±1 cm	Detection range	300 m
Absolute accuracy	≤5 cm	RTK accuracy	1 cm + 1 ppm

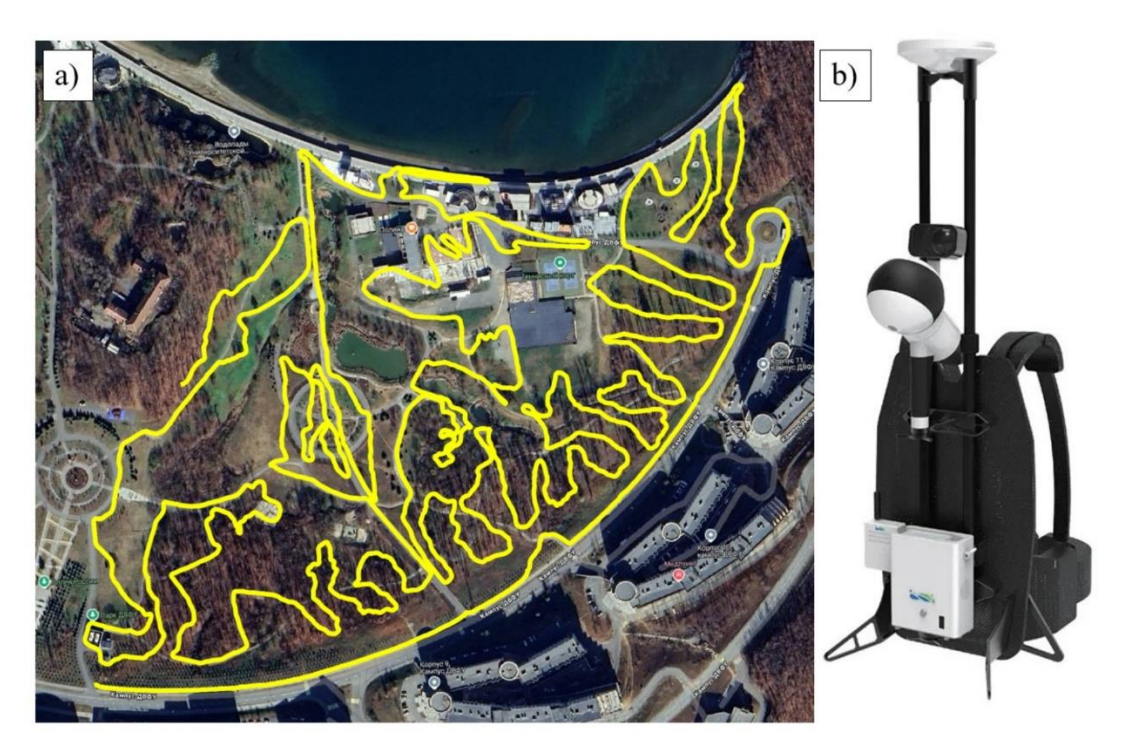


Figure 5.
Trajectory of ground-based laser scanning.
Note: a. Trajectory of movement with the device. b. Laser scanner GreenValley LiGrip H300 with backpack.

2.3. Research Methods

The algorithm consisted of using aerial (multispectral, LiDAR) and ground LiDAR survey field data. Where the multispectral orthophoto is classified by tree species, the ground and air point clouds are combined to determine the height of the tree and the diameter of the trunk. The obtained data are compared with field observations in the test area. After that, biomass is calculated for individual trees, then for individual species.

2.3.1. Getting Attribute Information about Individual Trees

To identify trees, it is necessary to perform a procedure for clearing the point cloud from noise, classify the points of the earth's surface. Then, using the Lidar360 software machine learning functions, classify objects by type and vegetation height. After that, it is necessary to normalize the point cloud to bring it to a single elevation, since the relief of the site under study has significant differences, which prevent the correct processing of the point cloud. Next, using the TLS seed point editor function, the parameters were determined by which trees would be selected from the point cloud. Minimal DBH 10 cm, maximum 2 meters, with an angle of deviation from the ground of no more than 30°. To get detailed information about the height and diameter of each tree, you need to combine two point clouds. As a result of processing the data from aerial and ground laser scanning, point clouds were obtained, the profiles of which are shown in Figure 6.

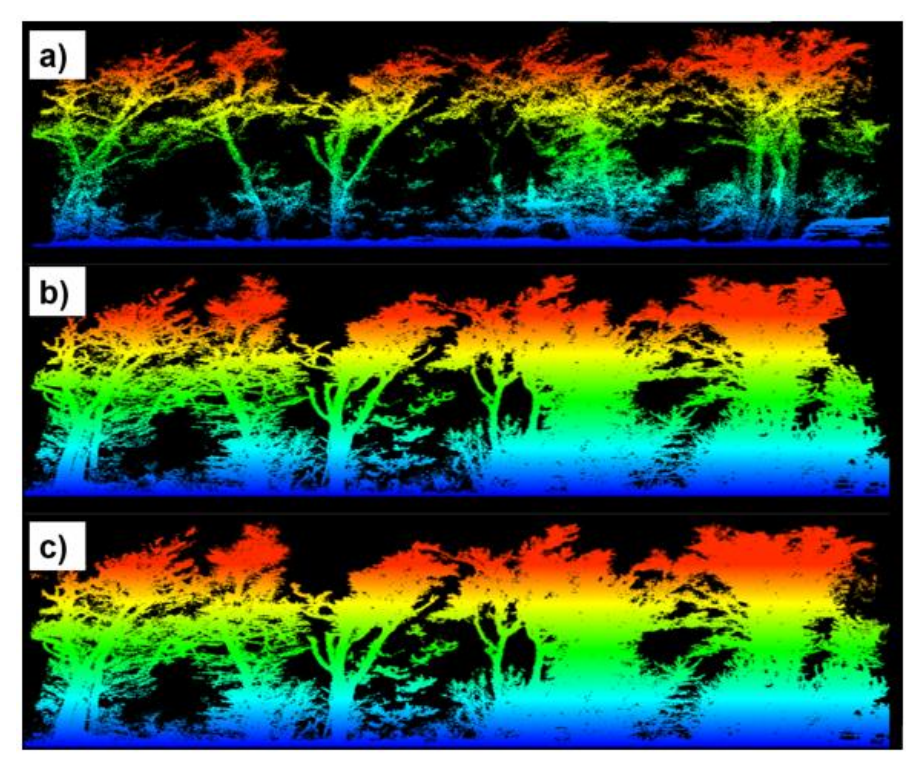


Figure 6.
Laser scanning profiles
a. Aerial scanning, b. Ground scanning, c. Combined point clouds.

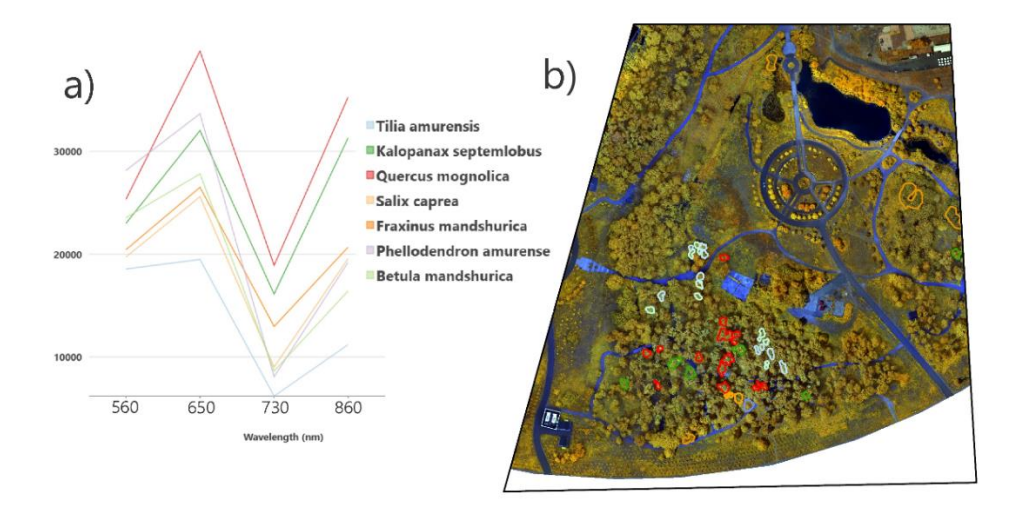
Vegetation profiles show that the boundaries of tree trunks are well contoured in both point clouds, but ground laser scanning contains more information. There is noise in aerial laser scanning, and it is also impossible to distinguish the contours of tree trunks, but the crowns are presented with high detail. In ground-based laser scanning, the contours are clear, and the point cloud contains enough information for analysis. After processing the laser scan, attribute information (coordinates, diameter (DBH), height, area, canopy shape) was extracted from the combined point cloud. To verify the correctness of the point cloud segmentation function, a 20*20 m site was selected, where geobotanical descriptions were carried out. Eighteen trees (seven species) were identified at the test site using reconnaissance, and the tree height and DBH parameters were determined using field methods.

2.3.2. Determining tree species

To calculate the biomass of individual trees in complex plantings, in addition to the obtained attributes, it is necessary to determine the type of tree. The multispectral survey was carried out by UAV DJI Mavic 3 Multispectral, which is equipped with two cameras: RGB and a multispectral camera. The multispectral camera has 4 lenses on 5 MP 1/2.8-inch image sensors configured to work in the following ranges of the electromagnetic spectrum: green (560 ± 16 nm), red (650 ± 16 nm), red edge (730 ± 16 nm), and near infrared (860 ± 16 nm).

The aerial photography results were processed in Agisoft Metashape software with the preparation of orthophotography images with a spatial resolution of 3 cm/pixel. To classify plant species, a training sample of 11 classes of trees was created. It was formed both based on the results of a field survey and on the basis of expert interpretation of orthophotography images. At the same time, the type of plant was determined by an expert based on differences in the architecture of the trees.

The classification was performed using the «Random Forest» algorithm. Previously, a mask was applied to the multichannel raster, from which all objects not related to vegetation were excluded by determining the NDVI (Figure 7).



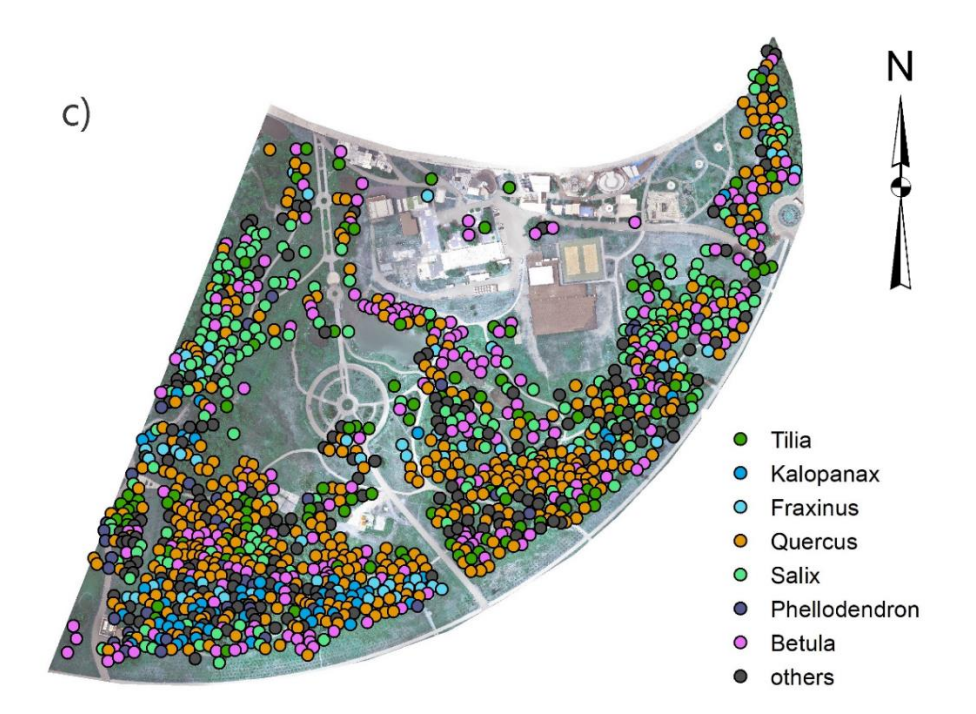


Figure 7.

The procedure for determining the type of tree based on multispectral data.

Note: a. Spectral profile of the main tree species,

b. Polygons of the training sample in the image in pseudo-colors (near infrared – red edge – red), c. Results of the classification of trees by species.

The classification results were evaluated using metrics such as overall accuracy, accuracy for the map user, accuracy for the map creator, and F1 scores. In this case, an n*n square matrix is used as the basis, where n is the number of classes (the inconsistency matrix).

Then the classification results were combined with information about the location and projective cover of tree canopies obtained from laser scanning.

The combination of multispectral aerial photography, ground-based, and aerial laser scanning makes it possible to obtain attribute information for individual trees, which is used to calculate biomass.

2.3.3. Calculation of Biomass of Individual Trees After Classification

To calculate the individual biomass of a tree, it is necessary to obtain the following values: the diameter of the trunk at a height of 1.3 m, the height of the tree, and the type of tree.

For calculating the volume of the studied territory, using the binary volumetric model of a separate tree: $V = aD^bH^c$

Where:

- a, b, c parameters of model [23]
- D DBH
- H tree height

Total aboveground biomass is calculated using the formula $Wt = f(D^{\rho}H)^{\delta}$. Underground biomass Wr = Wt/3.85, total biomass W = Wt + Wr.

According to the algorithm presented above, the types of trees on the site were classified using multispectral data combined with laser scanning. Data was calibrated based on the results of field geobotanical work. Individual characteristics were obtained for each tree, on the basis of which the biomass of each tree species was calculated.

3. Results and Discussion

3.1. Calculation Based on a Combination of Three Types of Surveys

As a result of laser scanning, 1255 trees were identified in the territory, among which 679 trees with a diameter of more than 10 cm were selected for further processing. All 7 species described in the trial area are represented among the selected trees (Table 1). Based on the point cloud, attribute information (coordinates, height, DBH) about each tree is obtained. Table 5 shows a comparison of the results of field geobotanical work with laser scanning.

Table 5.Comparison of DBH and tree height based on field data and ground scanning.

Tree species	Height /m (field)	Height /m (scanning)	dHeight /m	dHeight /%	DBH /cm (field)	DBH /cm (scanning)	dDBH /cm	dDBH /%
Salix caprea	18.5	20.5	-2	9.8	41.4	44.6	-3.2	7.7
Phellodendron amurense	6	6.2	-0.2	3.2	16.9	15.9	1	5.9
Fraxinus mandshurica	23	25.7	-2.7	10.5	43.9	39.9	4	9.1
Quercus mongolica	13.5	15	-1.5	10	25.9	23.1	2.8	10.8
Kalopanax septemlobus	16	17.8	-1.8	10.1	60	56.1	3.9	6.4
Betula mandshurica	16	17.6	-1.6	9.1	36.8	33.1	3.7	10.1
Tilia amurensis	18	19.7	-1.7	8.6	23.1	23.8	-0.8	3.3

The table shows that the difference in the definitions of heights and diameters is no more than 11%. It is worth noting that field measurements of tree heights tend to decrease in accuracy with increasing

Edelweiss Applied Science and Technology ISSN: 2576-8484

ISSN: 2576-8484

Vol. 9, No. 10: 1552-1566, 2025 DOI: 10.55214/2576-8484.v9i10.10701

DOI: 10.55214/2576-8484.v9i10.10701 © 2025 by the authors; licensee Learning Gate height, which is due to the peculiarities of the measurement method. While laser scanning has no restrictions in determining the height of a tree, especially when using a combined point cloud with parallel use of a positioning base station and identification marks. In this case, field measurements of tree heights are not used for calculations. The difference in tree diameters is no more than 4 cm, while for individuals of some species (Phellodendron, Tilia), the difference does not exceed 1 cm, which is due to the peculiarity of the trunk configuration and the location of the tree relative to dense vegetation.

Cross-validation of tree species was performed through a stratified random sample. At the same time, 500 points were randomly distributed in proportion to the projective cover (area) of the canopy. The true value of the tree species was determined by an expert using orthophotography images and field surveys. The F1 metric has been adopted as the main accuracy criterion, which varies from 0 to 1. It can be interpreted as the average harmonic mean of the metrics of overall accuracy (OA) and accuracy from the point of view of the map creator (Producer accuracy, PA).

The overall accuracy of the cross-validation was 63.3%. For the Tilia and Kalopanax classes, the F1 metric exceeded 0.8. For other classes, it is significantly lower, with the highest number of errors occurring in Betula (0.45) and Fraxinus (0.54) classes.

3.2. Biomass calculation for individual tree species

The results of biomass calculations for individual tree species are presented in Table 6.

Table 6. Results of calculating the biomass of tree species.

Tree species	Volume/m ³	Wt/kg	Wr/kg	W
Tilia	97.67	12,237.08	3,178.46	15,415.54
Kalopanax	98.89	22,366.85	5,809.57	28,176.42
Fraxinus	74.66	17,471.61	4,538.08	22,009.69
Quercus	263.79	81,069.59	21,057.04	102,126.63
Salix	126.32	79,405.61	20,624.83	100,030.45
	31.56	3,465.66	900.17	4,365.84
Betula	124.56	17,498.52	4,545.07	22.043.59
Other	210.95	120,456.49	31,287.4	15,1743.89

The table shows that the largest volume of wood and biomass reserves at the carbon polygon is concentrated in the following species: Quercus, Salix, Betula. According to the classification, the total number for the three predominant species is 426 trees, which together occupy a volume of 514.67 m³. The smallest volume of wood and biomass reserves is represented by 90 trees with species: Phellodendron, Tilia, Fraxinus, with a total volume of 203.89 m³.

4. Conclusion

As a result of a complex of works on ground and aerial laser scanning and multispectral aerial photography, 1255 trees were identified on the territory of the Far Eastern carbon polygon (Ajax Bay), of which 679 trees were studied, among which Quercus mongolica prevails. Using the proposed combined algorithm (multispectral orthophoto images for species detection, combined point cloud of ground and aerial laser scanning for determination of quantitative parameters of individual trees), the following parameters were determined: location, trunk diameter, height of tree, tree species, volume, and biomass. The data has been refined based on field geobotanical studies of the test area. The accuracy of determining species is 63%, the accuracy of determining height of tree is 5-10 cm, the accuracy of determining diameter (requires additional study) is 1-4 cm. Of the trees represented on the site, Tilia and Kalopanax are identified by the proposed algorithm better than others. The most accurate diameters were obtained for single standing trees with a diameter more than 10 cm. Thus, the described combined method has a number of advantages over the field method; it is slightly inferior in accuracy but allows

Vol. 9, No. 10: 1532-1566, 2025

DOI: 10.55214/2576-8484.v9i10.10701

© 2025 by the authors; licensee Learning Gate

quick acquisition of information about parameters of mixed forests for operational and seasonal biomass calculation.

In complex forest plantings, multispectral methods can be used to determine tree species. For the estimation of individual tree parameters, LiDAR technology can be employed. The precise combination of these two types of data makes it possible to recognize tree species and calculate the biomass of individual trees in difficult forest conditions.

Funding:

The work was carried out with the financial support of the Ministry of Science and Higher Education of the Russian Federation (Grant Number: FZNS-2025-0004) "Assessment of the sequestration potential of coastal marine ecosystems".

Transparency:

The authors confirm that the manuscript is an honest, accurate, and transparent account of the study; that no vital features of the study have been omitted; and that any discrepancies from the study as planned have been explained. This study followed all ethical practices during writing.

Copyright:

© 2025 by the authors. This article is an open-access article distributed under the terms and conditions of the Creative Commons Attribution (CC BY) license (https://creativecommons.org/licenses/by/4.0/).

References

- [1] R. A. Hember and W. A. Kurz, "Low tree-growth elasticity of forest biomass indicated by an individual-based model," Forests, vol. 9, no. 1, p. 21, 2018. https://doi.org/10.3390/f9010021
- D. J. Krofcheck, M. E. Litvak, C. D. Lippitt, and A. Neuenschwander, "Woody biomass estimation in a southwestern US juniper savanna using LiDAR-derived clumped tree segmentation and existing allometries," *Remote Sensing*, vol. 8, no. 6, p. 453, 2016. https://doi.org/10.3390/rs8060453
- [3] K. Stereńczak et al., "Factors influencing the accuracy of ground-based tree-height measurements for major European tree species," Journal of Environmental Management, vol. 231, pp. 1284-1292, 2019. https://doi.org/10.1016/j.jenvman.2018.09.100
- [4] E. F. Berra, R. Gaulton, and S. Barr, "Assessing spring phenology of a temperate woodland: A multiscale comparison of ground, unmanned aerial vehicle and Landsat satellite observations," *Remote Sensing of Environment*, vol. 223, pp. 229-242, 2019. https://doi.org/10.1016/j.rse.2019.01.010
- [5] C. Anjin, Y. Kim, Y. Kim, and Y. Eo, "Estimation of individual tree biomass from airborne lidar data using tree height and crown diameter," *Disaster Advances*, vol. 5, no. 4, pp. 360-365, 2012.
- [6] A. A. Borsah, M. Nazeer, and M. S. Wong, "LIDAR-based forest biomass remote sensing: A review of metrics, methods, and assessment criteria for the selection of allometric equations," *Forests*, vol. 14, no. 10, p. 2095, 2023. https://doi.org/10.3390/f14102095
- [7] L. Cao, H. Liu, X. Fu, Z. Zhang, X. Shen, and H. Ruan, "Comparison of UAV LiDAR and digital aerial photogrammetry point clouds for estimating forest structural attributes in subtropical planted forests," *Forests*, vol. 10, no. 2, p. 145, 2019. https://doi.org/10.3390/f10020145
- [8] J. Lisein, M. Pierrot-Deseilligny, S. Bonnet, and P. Lejeune, "A photogrammetric workflow for the creation of a forest canopy height model from small unmanned aerial system imagery," *Forests*, vol. 4, no. 4, pp. 922-944, 2013. https://doi.org/10.3390/f4040922
- [9] W. Li, Q. Guo, M. K. Jakubowski, and M. Kelly, "A new method for segmenting individual trees from the lidar point cloud," *Photogrammetric Engineering & Remote Sensing*, vol. 78, no. 1, pp. 75-84, 2012. https://doi.org/10.14358/PERS.78.1.75
- [10] R. Neuville, J. S. Bates, and F. Jonard, "Estimating forest structure from UAV-mounted LiDAR point cloud using machine learning," *Remote Sensing*, vol. 13, no. 3, p. 352, 2021. https://doi.org/10.3390/rs13030352
- [11] A. T. Hudak, A. T. Haren, N. L. Crookston, R. J. Liebermann, and J. L. Ohmann, "Imputing forest structure attributes from stand inventory and remotely sensed data in western Oregon, USA," *Forest Science*, vol. 60, no. 2, pp. 253-269, 2014. https://doi.org/10.5849/forsci.12-101
- [12] A. Safonova et al., "Individual tree crown delineation for the species classification and assessment of vital status of forest stands from UAV images," *Drones*, vol. 5, no. 3, p. 77, 2021. https://doi.org/10.3390/drones5030077

- [13] M. Dalponte and D. A. Coomes, "Tree-centric mapping of forest carbon density from airborne laser scanning and hyperspectral data," *Methods in Ecology and Evolution*, vol. 7, no. 10, pp. 1236-1245, 2016. https://doi.org/10.1111/2041-210X.12575
- [14] F. Brieger, U. Herzschuh, L. A. Pestryakova, B. Bookhagen, E. S. Zakharov, and S. Kruse, "Advances in the derivation of Northeast Siberian forest metrics using high-resolution UAV-based photogrammetric point clouds," *Remote Sensing*, vol. 11, no. 12, p. 1447, 2019. https://doi.org/10.3390/rs11121447
- [15] A. S. Alekseev, Y. I. Danilov, A. A. Nikiforov, M. E. Guzyuk, and D. M. Kireev, "Experience in unmanned air vehicle application for inventory and assessment of experimental forest plantations in the Lisinsk part of the training-and-experimental forestry of the Leningrad Region," *Proceedings of the St. Petersburg Scientific Research Institute of Forestry*, vol. 2, pp. 46–48, 2020.
- N. V. Ivanova, M. P. Shashkov, and V. N. Shanin, "Determination of characteristics of mixed stands based on aerial photography using an unmanned aerial vehicle (UAV). Vestnik Tomskogo Gosudarstvennogo Universiteta," Biologiya / Tomsk State University Journal of Biology, vol. 54, pp. 158–175, 2021.
- Y. Pu, D. Xu, H. Wang, X. Li, and X. Xu, "A new strategy for individual tree detection and segmentation from leaf-on and leaf-off UAV-LiDAR point clouds based on automatic detection of seed points," *Remote Sensing*, vol. 15, no. 6, p. 1619, 2023. https://doi.org/10.3390/rs15061619
- V. A. Kostyk, I. A. Lisina, and S. V. Vikhrenko, "Climatic conditions of functioning of carbon polygons in the south of Primorsky Krai. In Soil and carbon-saving technologies in the agro-industrial complex of Russia and the world," in *International Scientific Conference Proceedings (pp. 60–64). Moscow, Russia*, 2024.
- [19] Far Eastern Carbon Landfill, "Far Eastern Carbon Landfill," 2024. https://carbon-polygons.ru/
- V. N. Sukachev, S. V. Zonn, and Z. P. Motovilov, Methodological guidelines for the study of forest types. Moscow: Publishing House of the USSR Academy of Sciences, 1957.
- [21] T. A. Worknov, *Phytocenology*, 2nd ed. Moscow: Moscow State University, 1983.
- [22] S. S. Kharkevich, Vascular plants of the soviet far East. St. Petersburg: Nauka, 1997.
- X. Lian *et al.*, "Biomass calculations of individual trees based on unmanned aerial vehicle multispectral imagery and laser scanning combined with terrestrial laser scanning in complex stands," *Remote Sensing*, vol. 14, no. 19, p. 4715, 2022. https://doi.org/10.3390/rs14194715